$$k = \mathscr{F}^{-1}[\mathscr{F}J_1 \cdot \mathscr{F}^* J_2]. \tag{2.5.5.27}$$

The probability density of samples for images has the form

$$p(J_1 J_2 \ldots J_n) = \frac{1}{(\sigma\sqrt{2\pi})^n} \times \exp\left[\frac{-1}{2\sigma^2}\sum^{n}\int [J_k(\mathbf{x}+\mathbf{x}_k) - J(\mathbf{x})]^2 \, \mathrm{d}x\right]. \tag{2.5.5.28}$$

Here J is the tentative image (as such, a certain 'best' image can first be selected, while at the repeated cycle an average image is obtained), $J_k(\mathbf{x})$ is the image investigated, σ is the standard deviation of the normal distribution of noises and x_k the relative shift of the image. This function is called a likelihood function; it has maxima relative to the parameters $J(x)$, x_k, σ. The average image and dispersion are

$$J(\mathbf{x}) = (1/n)\sum^{n}[J_k(\mathbf{x}-\mathbf{x}_k)],$$
$$\sigma^2 = (1/n)\sum^{n}[J_k(\mathbf{x}-\mathbf{x}_k) - J(\mathbf{x})]^2. \tag{2.5.5.29}$$

This method is called the maximum-likelihood method (Cramér, 1954; Kosykh *et al.*, 1983).

It is convenient to carry out the image alignment, in turn, with respect to translational and angular coordinates. If we start with an angular alignment we first use autocorrelation functions or power spectra, which have the maximum and the symmetry centre at the origin of the coordinates. The angular correlation maximum

$$f(\theta') = \int f_k(\theta - \theta') f_e(\theta) \, \mathrm{d}\theta \tag{2.5.5.30}$$

gives the mutual angle of rotation of two images.

Then we carry out the translational alignment of rotationally aligned images using the translational correlation function (2.5.5.26) (Langer *et al.*, 1970).

In the iteration alignment method, the images are first translationally aligned and then an angular shift is determined in image space in polar coordinates with the centre at the point of the best translational alignment. After the angular alignment the whole procedure may be repeated (Steinkilberg & Schramm, 1980).

The average image obtained may have false high-frequency components. They can be excluded by multiplying its Fourier components by some function and suppressing high-space frequencies, for instance by an 'artificial temperature factor' $\exp\{-B|\mathbf{u}|^2\}$.

For a set of similar images the Fourier filtration method can also be used (Ottensmeyer *et al.*, 1977). To do this, one should prepare from these images an artificial 'two-dimensional crystal', *i.e.* place them in the same orientation at the points of the two-dimensional lattice with periods a, b.

$$J = \sum_{k=1}^{n} J_k(\mathbf{x} - \mathbf{t}_p); \; \mathbf{t} = p_1\mathbf{a} + p_2\mathbf{b}. \tag{2.5.5.31}$$

The processing is then performed according to (2.5.5.18), (2.5.5.19); as a result one obtains $\langle I(xy)\rangle$ with reduced background. Some translational and angular errors in the arrangement of the images at the artificial lattice points act as an artificial temperature factor. The method can be realized by computing or by optical diffraction.

2.5.6. Three-dimensional reconstruction[5]

By B. K. Vainshtein and P. A. Penczek

2.5.6.1. The object and its projection

In electron microscopy (EM) and single-particle reconstruction, three-dimensional (3D) reconstruction methods are used for studying biological structures; that is, symmetric or asymmetric associations of biomacromolecules (muscles, spherical and rod-like viruses, bacteriophages, individual proteins and ribosomes) (Frank, 2006). The electron microscope is used to obtain parallel-beam two-dimensional (2D) projections $\varphi_2(\mathbf{x}, \boldsymbol{\tau})$ (ray transform) of frozen hydrated 3D macromolecules $\varphi_3(\mathbf{r})$ suspended in random orientations (Fig. 2.5.6.1). The function $\varphi_2(\mathbf{x}_\tau)$ is the 2D projection of the 3D molecular electron distribution $\varphi_3(\mathbf{r})$. One can also consider one-dimensional (1D) projections $\varphi_1(s, \boldsymbol{\tau})$ of multidimensional distributions; the set of these projections is called a Radon transform. For 2D distributions, ray and Radon transforms differ only in the notation. For $(d > 2)$-dimensional distributions the two are different: in a ray transform the integrals are calculated over straight lines and yield $(d-1)$-dimensional projections, while in Radon transforms the integrals are calculated over $(d-1)$-dimensional hyperplanes and yield 1D projections. In electron microscopy, Radon transforms are not directly measurable, but can be formed computationally and used in intermediate steps of the 3D reconstruction or in alignment procedures (Radermacher, 1994).

Within the linear weak-phase-object approximation of the image-formation process in the microscope [see equation (2.5.2.42) in Section 2.5.2 of this chapter], 2D projections represent line integrals of the potential of the particle under examination convoluted with the point-spread function of the microscope, s, so, using (2.5.2.43),

$$I(xy) = 1 + 2\sigma s(xy) * \varphi(xy) = 1 + 2\sigma s(xy) * \int \varphi_3(\mathbf{r}) \, \mathrm{d}z. \tag{2.5.6.1}$$

Since

$$\varphi_2(\mathbf{x}_\tau) = \int \varphi_3(\mathbf{r}) \, \mathrm{d}\tau, \quad \boldsymbol{\tau} \perp \mathbf{x}, \tag{2.5.6.2}$$

we have

$$I(xy) = 1 + 2\sigma s(\mathbf{x}_\tau) * \varphi_2(\mathbf{x}_\tau), \quad \boldsymbol{\tau} \perp \mathbf{x}. \tag{2.5.6.3}$$

If we omit constant terms, we obtain

$$I(xy) = s(\mathbf{x}_\tau) * \varphi_2(\mathbf{x}_\tau) = s(\mathbf{x}_\tau) * \int \varphi_3(\mathbf{r}) \, \mathrm{d}\tau, \quad \boldsymbol{\tau} \perp \mathbf{x}. \tag{2.5.6.4}$$

In this section, we will assume that all images were collected using the same defocus setting, so the point-spread function s is constant and does not depend on the projection direction $\boldsymbol{\tau}$. Thus, we will concern ourselves with the inversion of the projection problem

$$\varphi_2(\mathbf{x}_\tau) = \int \varphi_3(\mathbf{r}) \, \mathrm{d}\tau, \quad \boldsymbol{\tau} \perp \mathbf{x}. \tag{2.5.6.5}$$

[5] The original version of Section 2.5.6, written by the late B. K. Vainshtein, is here updated and expanded by P. A. Penczek.

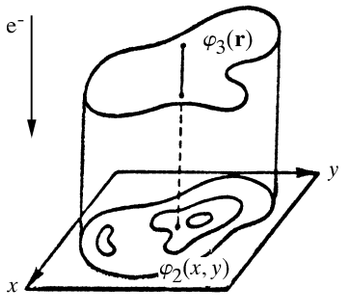

Fig. 2.5.6.1. A three-dimensional object φ_3 and its two-dimensional projection φ_2. The electron beam penetrates the specimen in the direction of the z axis.

The projection direction is defined by a unit vector $\boldsymbol{\tau}(\theta, \psi)$ and it is formed on the plane $\mathbf{x}$ perpendicular to $\boldsymbol{\tau}$. The set of various projections $\varphi_2(\mathbf{x}_{\tau_i}) = \varphi_{2_i}(\mathbf{x}_i)$ may be assigned by a discrete or continuous set of points on a unit sphere $|\tau| = 1$ (Fig. 2.5.6.2).

In Fourier space, the relation between an object and its projection is referred to as the central section theorem: the Fourier transformation of projection φ_2 of a 3D object φ_3 is the central (*i.e.*, passing though the origin of reciprocal space) 2D plane cross section of a 3D transform perpendicular to the projection vector (Bracewell, 1956; DeRosier & Klug, 1968; Crowther, Amos *et al.*, 1970). In Cartesian coordinates, a 3D Fourier transform is

$$\begin{aligned}\mathscr{F}[\varphi_3(\mathbf{r})] &= \Phi_3(u, v, w) \\ &= \iiint \varphi_3(x, y, z) \exp\{2\pi i(ux + vy + wz)\}\, \mathrm{d}x\, \mathrm{d}y\, \mathrm{d}z.\end{aligned} \tag{2.5.6.6}$$

The transform of projection $\varphi_2(x, y)$ along z is

$$\begin{aligned}\mathscr{F}[\varphi_2(x, y)] &= \Phi_3(u, v, 0) \\ &= \iiint \varphi_3(x, y, z) \exp\{2\pi i(ux + vy + 0z)\}\, \mathrm{d}x\, \mathrm{d}y\, \mathrm{d}z \\ &= \iiint \varphi_3(x, y, z)\, \mathrm{d}z \exp\{2\pi i(ux + vy)\}\, \mathrm{d}x\, \mathrm{d}y \\ &= \iint \varphi_2(x, y) \exp\{2\pi i(ux + vy)\}\, \mathrm{d}x\, \mathrm{d}y \\ &= \Phi_2(u, v).\end{aligned} \tag{2.5.6.7}$$

In the general case of projecting along the vector $\boldsymbol{\tau}$, the central section theorem is

$$\mathscr{F}[\varphi_2(\mathbf{x}_\tau)] = \Phi_3(\mathbf{u}_\tau), \quad \mathbf{u}_\tau \perp \boldsymbol{\tau}. \tag{2.5.6.8}$$

From this theorem it follows that the inversion of the 3D ray transform is possible if there is a continuous set of projections φ_τ corresponding to the motion of the vector $\boldsymbol{\tau}(\theta, \psi)$ over any continuous line connecting the opposite points on the unit sphere (Fig. 2.5.6.2) (Orlov's condition: Orlov, 1976). This result is evidenced by the fact that in this case the cross sections $\mathscr{F}[\varphi_2(\mathbf{x}_\tau)]$ that are perpendicular to $\boldsymbol{\tau}$ in Fourier space continuously cover the whole Fourier space, *i.e.*, they yield $\mathscr{F}[\varphi_3(\mathbf{r})]$ and thereby determine $\varphi_3(\mathbf{r}) = \mathscr{F}^{-1}[\Phi_3(\mathbf{u})]$.

In single-particle reconstruction, imaged objects are randomly and nonuniformly oriented on the substrate at different angles (Frank, 2006) and the distribution of their orientations is beyond our control; therefore, the practical impact of Orlov's condition is limited. In fact, it is more useful to determine *a posteriori*, *i.e.*, after the 3D reconstruction of the macromolecule is computed, how well the Fourier space was covered. This can be done by calculating the distribution of the 3D spectral signal-to-noise ratio (Penczek, 2002).

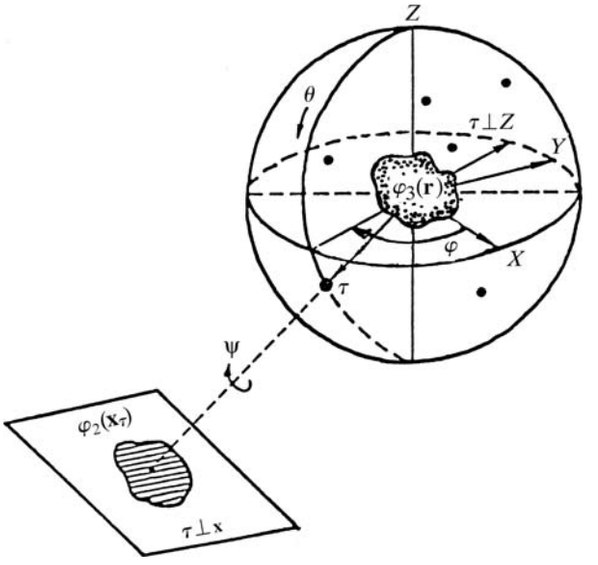

Fig. 2.5.6.2. The projection sphere and projection $\varphi_2(\mathbf{x}_\tau)$ of $\varphi_3(\mathbf{r})$ along $\boldsymbol{\tau}$ onto the plane $\boldsymbol{\tau} \perp \mathbf{x}$. The case $\boldsymbol{\tau} \perp Z$ represents orthoaxial projection. Points indicate an arbitrary distribution of projection directions $\boldsymbol{\tau}$.

2.5.6.2. 3D reconstruction in the general case

In the general case of the 3D reconstruction of $\varphi_3(\mathbf{r})$ from projections $\varphi_2(\mathbf{x}_\tau)$, the projection vector $\boldsymbol{\tau}$ occupies arbitrary positions on the projection sphere (Fig. 2.5.6.2). First, let us consider the case of a 2D function $\rho_2(\mathbf{x})$ and its ray transform $\varphi_1(x, \psi)$. We introduce an operation of backprojection b, which is stretching along $\boldsymbol{\tau}_\psi$ each 1D projection $\varphi_1(x_\psi)$ (Fig. 2.5.6.3). When the result is integrated over the full angular range of projections $\varphi_1(x, \psi)$, we obtain the projection synthesis defined as

$$b(x, y) = \int_0^\pi \varphi_1(x \cos\psi + y \sin\psi, \psi)\, \mathrm{d}\psi. \tag{2.5.6.9}$$

However, the backprojection operator is not the inverse of a 2D ray transform, as the resulting image b is blurred by the point-spread function $(x^2 + y^2)^{-1/2}$ (Vainshtein, 1971):

$$b(x, y) = \rho(x, y) * (x^2 + y^2)^{-1/2}. \tag{2.5.6.10}$$

By noting that the Fourier transform of $(x^2 + y^2)^{-1/2}$ is $(u^2 + v^2)^{-1/2}$ and by using the convolution theorem $\mathscr{F}[f * g] = \mathscr{F}[f]\mathscr{F}[g]$, we obtain the 'backprojection-filtering' inversion formula:

$$\begin{aligned}\rho(x, y) &= b(x, y) * (x^2 + y^2)^{1/2} = \mathscr{F}^{-1}\big[|\mathbf{u}|\mathscr{F}[b]\big] \\ &= \text{Filtration}_{|\mathbf{u}|}[\text{Backprojection}(\varphi_1)].\end{aligned} \tag{2.5.6.11}$$

The more commonly used 'filtered-backprojection' inversion is based on the 2D version of the central section theorem (2.5.6.8):

$$\mathscr{F}[\varphi_1(x_\psi)] = \Upsilon_2(\mathbf{u}_\psi) = \Upsilon_2(R, \Psi), \tag{2.5.6.12}$$

where $\mathscr{F}[\rho_2] = \Upsilon_2$. With this in mind, $\rho_2(\mathbf{x})$ can be related to its ray transform by evaluating the Fourier transform of ρ_2 in polar coordinates:

references